

# Surface Chemistry of Azomethane Adsorbed on Si(111)-7 × 7 Surface Studied by SR-Photoemission, HREELS, and STM

Ruth Klauser\*

Synchrotron Radiation Research Center, No. 1 R&D Road VI, Hsinchu 300, Taiwan

Y. Tai, Y. L. Chan, and T. J. Chuang

Center for Condensed Matter Sciences, National Taiwan University, Taipei 106, Taiwan

Received: October 22, 2002; In Final Form: December 2, 2002

The adsorption and thermal decomposition behavior of azomethane on the Si(111)-7 × 7 surface has been studied by high-resolution electron energy loss spectroscopy (HREELS), synchrotron radiation photoelectron spectroscopy (SR-PES) in the soft X-ray and UV photon energy ranges, and scanning tunneling microscopy (STM). It is found that at 90 K substrate temperature, azomethane is adsorbed largely intact in both *trans* and *cis* forms. The decomposition of the molecules starts at an annealing temperature around 200 K with N=N bond breaking, and at 300 K, a mixture of remaining intact azomethane, NCH<sub>x</sub>, and Si-NH<sub>x</sub> species is present on the surface with three distinct N 1s photoemission peaks. At this temperature, the Si-N species begins to appear as nitride, but no Si-C bonding is detected. Carbon dissociates from nitrogen and reacts directly with the Si surface above 400 K with CH<sub>3</sub> adsorption as an intermediate adspecies. The CH<sub>3</sub> adsorption is strongly enhanced if azomethane is thermally precracked prior to the exposure. At 700 K, all surface carbon and nitrogen are bonded to Si. The remaining hydrogen is desorbed at 1000 K, and Si-C and Si-N phases are formed. After it is annealed to 1500 K, photoemission features typical for the clean Si(111)-7 × 7 surface are immediately recovered. Si-C and Si-N species are desorbed, leaving a homogeneous but disordered surface with an underlying 1 × 1 structure, which transforms back into the 7 × 7 structure by forming characteristic triangular-shaped patterns as intermediate steps in the surface reconstruction process.

## 1. Introduction

Surface science studies of silicon surfaces have often been driven by the technological aspects in microelectronics. Therefore, it is not surprising that adsorption systems on Si have been historically dominated by investigations of hydrogen, oxygen, fluorine, and chlorine, which are important elements in Si material processing. In recent years, however, in search for new materials as potential candidates for nanodevices, an increasing number of investigations are dealing with the interaction of saturated and unsaturated hydrocarbons with the Si surface. Hydrocarbon molecules are an important carbon source for the growth of carbides and diamond films and can serve as a model system for the interaction of organic molecules with Si in regards to the development of molecular electronics and biochemical devices. On the other hand, the chemistry of hydrocarbons on metal surfaces has been an intense field of research for decades in order to understand and control catalytic reactions and to identify surface intermediates. A similar knowledge of the reaction with semiconductor surfaces is desirable particularly in the context of the increasingly important chemical approach to tailor future devices.

The interest in the surface chemistry of azomethane (CH<sub>3</sub>N=NCH<sub>3</sub>) is due in part to its potential as a methyl source, which can be produced by pyrolysis of the molecule.<sup>1</sup> Several groups have studied the adsorption and decomposition of azomethane on various metal surfaces, such as Mo,<sup>2</sup> Pt,<sup>3</sup> Cu,<sup>4</sup> Rh,<sup>5,6</sup> and

Pd.<sup>7</sup> The molecule predominantly adsorbs molecularly on clean metal surfaces at low temperatures, and in many cases, in opposition to the gas phase reaction, it decomposes thermally by nitrogen–nitrogen bond scission. This can be, however, altered by either surface modification as shown for oxygen-covered Rh(111)<sup>5</sup> or electronic excitation<sup>8</sup> leading to a carbon–nitrogen dissociation of azomethane. Essential differences in the reaction can also occur depending on the surface structure. Whereas for the Cu(111) surface the molecule adsorbs at 90 K and desorbs molecularly at 190 K, both N=N and C–N bond breakings have been observed for the (110) face.<sup>4</sup> An important aspect for the surface reactivity is the initial adsorption symmetry of the molecule. In the majority of the cases where decomposition of the molecule has been reported, the initial *trans*-azomethane converts via isomerization to *cis*-azomethane and bonds through the nitrogen lone pairs to the surface. On Pd(111) and Rh(111), however, azomethane adsorbs in its *trans* configuration prior to the thermal decomposition.

There exist a few examples of azomethane adsorption on nonmetallic surfaces, namely, on Si(100),<sup>9</sup> diamond C(111),<sup>10</sup> and oxide surfaces.<sup>11</sup> The investigation on Si(100) showed that the molecule could adsorb at room temperature as both molecular and dissociated species. At higher temperatures, complete dissociation occurred and silicon carbide and nitride phases were observed. On the diamond surface, azomethane was found to be adsorbed intact at low temperature and completely desorbed at 200 K. The reaction with the oxide surfaces, although not under ultrahigh vacuum (UHV) conditions, was reported to be rather complex and might involve OH bridge

\* To whom correspondence should be addressed. Fax: +886 3-578-3813. E-mail: klauser@src.gov.tw.

bonding, as well as surface rearrangements such as tautomerization of azomethane into formaldehyde methylhydrazone ( $\text{CH}_2=\text{N}-\text{NH}-\text{CH}_3$ ). Such a transformation was also observed in some of the metal surface studies.<sup>3</sup>

The behavior of small molecules containing carbon and/or nitrogen on Si(100) and Si(111) surfaces is of fundamental interest not only because it is related to SiC, SiN, and organic layer thin film growth but also because it can provide important insight into the modification caused by adsorbates to the structural and electronic properties of the clean silicon surface. Particularly because of the advanced techniques of scanning tunneling microscopy (STM) and high-resolution X-ray photoelectron spectroscopy (HRXPS), the complicated bonding configurations of the clean silicon surfaces have now been rather well-understood and found to be in good agreement with theoretical calculations. In the case of the chemisorption of acetylene ( $\text{C}_2\text{H}_2$ ) and ethylene ( $\text{C}_2\text{H}_4$ ) on Si(111)- $7 \times 7$  and Si(100)- $2 \times 1$  surfaces, the molecules were suggested to be adsorbed intact forming di- $\sigma$  type bonds to two Si atoms.<sup>12–14</sup> Some restructuring of the original Si atoms was detected at higher coverages.<sup>15</sup> The interaction of CN-containing species with Si surfaces has been widely studied by the group of M. C. Lin and co-workers, including computational modeling of these systems.<sup>16–19</sup> HCN was reported to form dimers and polymers on Si(100) and to decompose after annealing to 220 K to CN and HCNH adspecies.  $\text{C}_2\text{N}_2$  molecules were found to adsorb in side on geometry on Si(100) and (111) surfaces up to an annealing temperature of 650 and 550 K, respectively. Above that, NC–CN bond breaking could occur. Methylhydrazine ( $\text{CH}_3\text{N}_2\text{H}_3$ ) was observed with the N–N bond parallel to the Si(111)- $7 \times 7$  surface upon adsorption but with partial dissociation of hydrogen. Annealing to 650 K caused N–N bond breaking. For all of the three adsorbates HCN,  $\text{C}_2\text{N}_2$ , and  $\text{CH}_3\text{N}_2\text{H}_3$ , further annealing results in further decomposition and at a temperature above 800 K, only C and N species remain, forming Si–carbide and Si–nitride.

In this work, we have investigated the adsorption and thermal decomposition behavior of pristine azomethane and precracked azomethane on the Si(111)- $7 \times 7$  surface. To understand the interplay between adsorption geometry, electronic properties, and surface morphology, we utilized three different surface sensitive techniques, namely, high-resolution electron energy loss spectroscopy (HREELS), synchrotron radiation photoelectron spectroscopy (SR-PES) in the soft X-ray, and UV photon energy ranges and STM.

## 2. Experimental Section

The experiments were carried out in three separate UHV systems but following the same surface preparation and treatment procedures. We cleaned the Si(111) wafer sample (resistivity of 0.1 ohm/cm) by one of the standard methods to remove surface oxide and obtain an atomically flat surface. The sample was repeatedly annealed by direct current heating to 1250 °C for 90 s until the pressure during annealing did not rise beyond  $5 \times 10^{-10}$  Torr. The cleanliness of the surface was determined by the STM  $7 \times 7$  image with minimal defects, a sharp  $7 \times 7$  low-energy electron diffraction (LEED) pattern with low background intensity, the appearance of the characteristic surface state peaks in the valence band and Si 2p spectra, and a featureless background in the HREELS spectrum. The synthesis method of azomethane was described in previous publications.<sup>1</sup> The gas was introduced into the UHV chamber by a variable leak valve and a quartz dosing tube facing the sample. The purity of the gas was confirmed by a quadrupole mass spectrometer

(QMS). For the precracked azomethane experiments, the gas was guided through a heated zone of a high-temperature quartz nozzle. It has been shown previously that the conversion rate of azomethane into  $\text{CH}_3$  and  $\text{N}_2$  can be about 80% for a nozzle temperature of 1100 K.<sup>1</sup> For the HREELS measurements, the incident electron energy was fixed at 4.68 eV with an incident angle of 44°. All loss signals were collected in specular direction with an overall resolution of 3.5 meV (fwhm of the elastic peak).

The high-resolution SR-PES study was performed at the Synchrotron Radiation Research Center (SRRC) in Hsinchu using photons from three different beamlines, namely, LSGM, HSGM, and U5. The spectra were taken with a nine channeltron hemispherical electron energy analyzer with an energy resolution in most cases of about 0.3 eV. The energy scale was referenced to the Si 2p<sub>3/2</sub> “bulk” peak at 99.3 eV binding energy (BE) of the clean Si surface, and additionally, an Au reference sample was introduced as calibration of the Fermi edge. After subtraction of the secondary electron background (Shirley background), all core level peaks were fitted using Voigt peak profiles, i.e., the Si 2p spectra by doublets with a standard spin–orbit splitting and branching ratio of the Si 2p<sub>3/2</sub> and Si 2p<sub>1/2</sub> peak constituents of 0.61 and 2 eV, respectively.

The STM experiments were conducted with a commercial room temperature UHV STM/atomic force microscopy (AFM) system attached to a small preparation chamber for sample annealing and azomethane exposure. The STM tips were electrochemically etched tungsten wires.

The annealing temperatures of the sample were determined by a pyrometer and by a thermocouple attached to the sample holder. The accuracy of the temperature, in particular for the low-temperature range between 350 and 600 K, is within  $\pm 30$  K.

## 3. Results and Discussion

**3.1. HREELS Measurements.** Figure 1 shows a series of HREELS spectra for the clean and azomethane-exposed Si-(111)- $7 \times 7$  surface. The surface was held at 90 K for the initial exposure of 0.12 L ( $= 2 \times 10^{-9}$  Torr  $\times$  60 s) and during data taking after annealing to various temperatures ( $T$ ). The initial surface coverage is less than one monolayer (1 ML). The loss spectrum of the clean silicon ( $7 \times 7$ ) reconstructed surface, as confirmed by the LEED pattern, has a smooth and continuous background with no remaining hydrogen. After the gas dosage, characteristic vibrational bands emerge as listed in Table 1. In comparison to previous vibrational data of adsorbed and solid phase azomethane molecules,<sup>2–4,20,21</sup> the various bands at  $T = 90$  K can be assigned as follows: the two strong bands at 522 and 647  $\text{cm}^{-1}$  to CNN bend modes; the strongest peak of the spectrum at 956  $\text{cm}^{-1}$  and the smaller bands at 1040 and 1118  $\text{cm}^{-1}$  to  $\text{CH}_3$  rock modes; the peak at 1195  $\text{cm}^{-1}$  to CN stretch; the small peak at 1240  $\text{cm}^{-1}$  and the broad band with center at 1431  $\text{cm}^{-1}$  to  $\text{CH}_3$  deformation modes; the band at 1575  $\text{cm}^{-1}$  to N=N stretch mode; the small hump at 2061  $\text{cm}^{-1}$  to a loss peak from H–Si stretch; and the very broad band with structures ranging from 2900 to 3100  $\text{cm}^{-1}$  to  $\text{CH}_3$  and  $\text{CH}_x$  ( $x \leq 2$ ) stretch frequencies. The initial adsorption geometry of submonolayer azomethane has been discussed in the paper of Jentz et al.<sup>3</sup> for the isomerization of the molecule on the Pt(111) surface. Four highly symmetric geometries are possible,  $C_2$  and  $C_s$  for *trans*-azomethane and  $C_{2v}$  and  $C_s$  for *cis*-azomethane. Indicators for the *trans* form configuration include a strong absorption peak at 2911  $\text{cm}^{-1}$  and a weak intensity of the N=N stretch above 1500  $\text{cm}^{-1}$ . In our case, the intensities and the appearance of a number of bands clearly suggest that both forms, *trans* and *cis*,

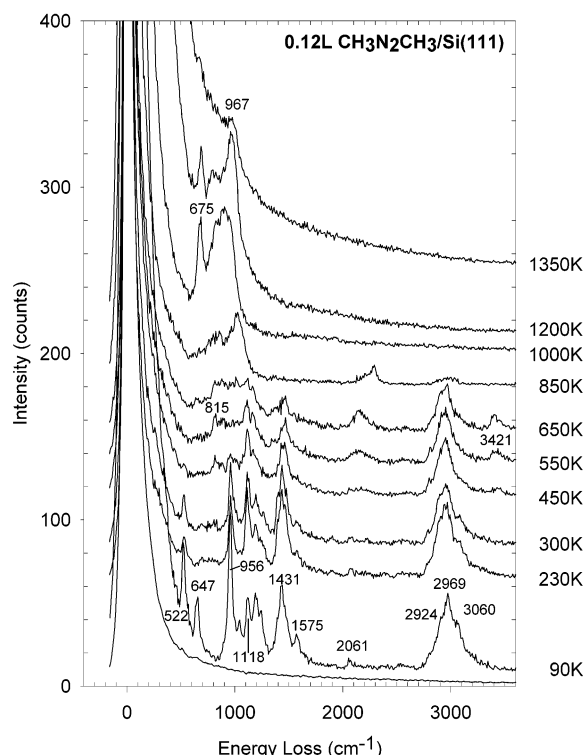


**Figure 1.** HREELS spectra for  $\text{CH}_3\text{N}_2\text{CH}_3$  on  $\text{Si}(111)-7 \times 7$  at various annealing temperatures ranging from 230 to 1350 K. The spectra were taken at 90 K with an initial exposure of 0.12 L. The bottom spectrum is the clean Si surface.

**TABLE 1:  $\text{CH}_3\text{N}_2\text{CH}_3/\text{Si}(111)-7 \times 7$  Vibrational Frequencies ( $\text{cm}^{-1}$ ) and Mode Assignments for Three Different Annealing Temperatures**

| 90 K   |  |      |  |
|--------|--|------|--|
| 522    | CNN bend ( $\delta$ -CNN)                              | 1431 | $\text{CH}_3$ deformation ( $\delta$ - $\text{CH}_3$ ) |
| 647    | CNN bend ( $\delta$ -CNN)                              | 1575 | $\text{N}=\text{N}$ stretch ( $\nu$ -NN)               |
| 956    | $\text{CH}_3$ rock ( $\delta$ - $\text{CH}_3$ )        | 2061 | $\text{Si}-\text{H}$ stretch                           |
| 1040   | $\text{CH}_3$ rock ( $\omega$ - $\text{CH}_3$ )        | 2924 | $\text{CH}_3$ stretch ( $\nu$ - $\text{CH}_3$ )        |
| 1118   | $\text{CH}_3$ rock ( $\rho$ - $\text{CH}_3$ )          | 2969 | $\text{CH}_3$ stretch ( $\nu$ - $\text{CH}_3$ )        |
| 1195   | CN stretch ( $\nu$ -CN)                                | 3060 | $\text{CH}_x$ stretch ( $\nu$ - $\text{CH}_x$ )        |
| 1240   | $\text{CH}_3$ deformation ( $\delta$ - $\text{CH}_3$ ) |      |  |
| 550 K  |  |      |  |
| 815    | $\text{Si}-\text{NCH}_x$                               | 1575 | $\text{N}=\text{N}$ stretch ( $\nu$ -NN)               |
| 880    | $\text{Si}-\text{NH}_x$                                | 2146 | $\text{Si}-\text{H}$ stretch                           |
| 1110   | $\text{CH}_x$ rock                                     | 2944 | $\text{CH}_x$ stretch                                  |
| 1167   | CN stretch   | 3421 | $\text{N}-\text{H}$ stretch                            |
| 1459   | $\text{CH}_x$ deformation                              |      |  |
| 1000 K |  |      |  |
| 675    | SiC  | 897  | SiN  |
| 772    | SiC  | 948  | SiN  |
| 832    | SiN  |      |  |

are present on the surface. The relative weak intensity at  $1575 \text{ cm}^{-1}$  and the appearance of bands at 2924, 1431, 1118, and  $522 \text{ cm}^{-1}$  matches well with the assignments for *trans*-azomethane of the solid phase and previous data. However, the strong intensities of peaks at 647 and  $956 \text{ cm}^{-1}$  and the presence of bands above  $3000 \text{ cm}^{-1}$  indicate that some of the molecules are likely to exist in the *cis* form on the surface. The small but noticeable peak at  $2061 \text{ cm}^{-1}$  due to the  $\text{Si}-\text{H}$  vibrational mode and the energy losses at 3060 and  $1240 \text{ cm}^{-1}$  further infer a small amount of hydrogen dissociation upon adsorption and the generation of  $\text{CH}_x$  species.

When the sample temperature is raised to 230 K, the intensities of the vibrational bands at 522, 647, 1195, and  $1575 \text{ cm}^{-1}$  decrease substantially. These peaks are related to CNN

and  $\text{N}=\text{N}$  vibrational modes, and the intensity changes clearly indicate that the molecule can dissociate by the breaking of a nitrogen–nitrogen bond at this temperature. Simultaneously, we observe an enhanced intensity at  $1115 \text{ cm}^{-1}$ , signaling the formation of  $\text{CH}_3$  and  $\text{NCH}_x$  adspecies. As the annealing temperature is increased above 300 K, molecular decomposition becomes more evident with new peaks emerging around 815 and  $880 \text{ cm}^{-1}$ . At  $T = 550 \text{ K}$ , the bands between 800 and  $900 \text{ cm}^{-1}$  gain in intensity and a new energy loss signal at  $3421 \text{ cm}^{-1}$  due to the  $\text{N}-\text{H}$  stretch mode demonstrates further dissociation of the adspecies, in particular the cracking of  $\text{C}-\text{N}$  bonds. In addition, more hydrogen cleavage is observed as a broad band centered at  $2146 \text{ cm}^{-1}$  from  $\text{Si}-\text{H}$  stretch. In the prior HREELS study<sup>22</sup> on the thermal behavior of  $\text{NH}_3$  on  $\text{Si}(111)-7 \times 7$ , the loss peak at  $835 \text{ cm}^{-1}$  was assigned to  $\nu(\text{Si}-\text{NH}_x)$ . This is consistent with the report of  $\text{CH}_3\text{N}_2\text{H}_3$  adsorption on the same surface,<sup>19</sup> where after annealing to 650 K a band at  $887 \text{ cm}^{-1}$  indicates the formation of  $\text{SiNH}_x$  and  $\text{SiNH}_x\text{CH}_y$ . Thus, our assignment of the observed bands near 815 and  $880 \text{ cm}^{-1}$  to  $\text{NCH}_x$  and  $\text{NH}_x$  should be quite reasonable. It is interesting to note that a weak signal near  $1575 \text{ cm}^{-1}$  is still visible at 650 K indicating that some residual  $-\text{N}=\text{N}-$  bonding has survived at this temperature.

Finally, after annealing to 1000 K, all bands above  $1000 \text{ cm}^{-1}$  are gone. The remaining strong signals with a sharp peak at  $675 \text{ cm}^{-1}$  and a broad band with center at  $897 \text{ cm}^{-1}$  can be attributed to  $\text{Si}$ -carbide and  $\text{Si}$ -nitride phases. In the reaction of  $\text{N}_2\text{H}_4$  with  $\text{Si}(111)-7 \times 7$ ,<sup>19</sup> the nitridation of the surface was observed to start with a broad band at  $968 \text{ cm}^{-1}$ , which at  $1000^\circ\text{C}$  annealing temperature was split into four bands at 500, 742, 992, and  $1089 \text{ cm}^{-1}$ . Those peaks can be related to  $\text{Si}_3\text{N}_4$  formation<sup>23</sup> in agreement with previous IR data on solid  $\text{Si}_3\text{N}_4$  showing a weak absorption peak at  $484 \text{ cm}^{-1}$  and strong peaks between 806 and  $1048 \text{ cm}^{-1}$ . Ammonia decomposition after hydrogen desorption was reported to show only two broad bands at 450 and  $900 \text{ cm}^{-1}$ , which were attributed to  $\text{Si}-\text{N}-\text{Si}$  stretching modes and  $\text{Si}_x\text{N}_y$  formation.<sup>22</sup> On the other hand, hydrocarbon adsorption on the  $7 \times 7$  reconstructed Si surface exhibited after SiC formation at elevated temperatures a vibrational signal at  $770 \text{ cm}^{-1}$ .<sup>14</sup> In the case of HCN, two bands appeared at 806 and  $1008 \text{ cm}^{-1}$  indicating SiC and SiN phases, similar to the reaction with  $\text{CH}_3\text{N}_2\text{H}_3$ , where those bands were located at 726 and  $967 \text{ cm}^{-1}$ , respectively. In the present study, we further observe that at  $T = 1200 \text{ K}$ , the broad band centered at  $897 \text{ cm}^{-1}$  sharpens to display discrete structures near 810 and  $970 \text{ cm}^{-1}$ , in addition to the peak at  $680 \text{ cm}^{-1}$ . We can conclude from the present observation and previous assignments that the higher frequency bands detected at  $T \geq 1000 \text{ K}$  are related to  $\text{Si}-\text{N}$  compounds, which form a single phase at higher annealing temperature, and the lower frequency band is due to SiC formation.

### 3.2. Photoemission Measurements. 3.2.1. Core Levels.

Figure 2 depicts a series of N 1s spectra of adsorbed azomethane taken at room temperature and at a photon energy of 512 eV for different dosages and sample annealing conditions. Except the last spectrum (d), all other spectra of nitrogen show a distinct structure of three peaks. For 1 L exposure at 300 K (Figure 2a), the three peaks are located at 400.3, 399.1, and  $397.8 \text{ eV}$  BE with a fwhm of the deconvoluted components of 1.1 eV. At a significantly larger exposure of 500 L at 300 K, increases in intensity of the signals at 400.1 and  $399.1 \text{ eV}$  of about 23% are observed and there is a reduction in intensity of the third peak at  $397.8 \text{ eV}$  of about 45%. This indicates that 1 L exposure is close to saturation coverage and no new species due to



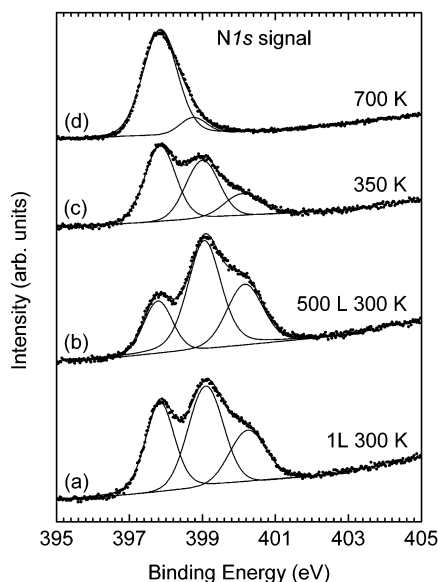


**Figure 2.** N 1s photoelectron spectra for  $\text{CH}_3\text{N}_2\text{CH}_3$  adsorbed on the  $\text{Si}(111)\text{-}7 \times 7$  surface taken at room temperature and at a photon energy of 512 eV: (a) 1 L adsorbed at 300 K, (b) 500 L adsorbed at 300 K, (c) 1 L adsorbed at 300 K and after annealing to 350 K, and (d) 1 L adsorbed at 300 K and after annealing to 700 K.

multilayer formation are apparent. The high BE peak around 400 eV is obviously related to pristine azomethane in the cis or trans form in agreement with the HREELS data. Similar N 1s BE have been detected for azomethane on  $\text{Si}(100)$ <sup>9</sup> and for  $\text{CH}_3\text{N}_2\text{H}_3$  on  $\text{Si}(111)\text{-}7 \times 7$ .<sup>19</sup> A slightly higher BE of 401.4 eV was reported in our previous study of azomethane adsorption on  $\text{Cu}(110)$ .<sup>24</sup> This is reasonable considering the weaker interaction of the molecule with the Cu surface. The second peak at 399 eV can be assigned to the cracking products of  $\text{NCH}_x$ . Similar to  $\text{Cu}(110)$ , a shift of 1.1 eV to lower BE from intact azomethane to  $\text{NCH}_x$  ( $x = 2, 3$ ) has also been observed. The lowest BE peak at 397.8 eV demonstrates further decomposition and the formation of the nitride phase, corresponding possibly to the form of  $\text{Si-NH}_x$  as identified in the HREELS spectra. The BE is close to the value from bulk  $\text{Si}_3\text{N}_4$  of 397.4 eV. Annealing to a temperature of only 350 K (Figure 2c) reduces drastically the peaks at 399 and 400 eV, whereas the 397.8 eV peak gains in intensity. The surface reaction includes desorption as well as further Si nitridation. At 700 K (Figure 2d) and higher  $T$ , Si-N remains essentially the only nitrogen-containing species on the surface, in agreement with the HREELS data.

Figure 3 shows the respective C 1s spectra acquired with the same photon energy of 512 eV. Although similar to N 1s, three components can be identified, the transformation with increasing annealing temperature occurs much faster in a smaller temperature range, reflecting the fact that carbon can only react with the silicon surface after detachment from nitrogen. At 1 L room temperature exposure (Figure 3a), the spectrum is dominated by a peak at 285.9 eV BE with a small shoulder at 285.3 eV and tiny hump around 283.3 eV. All fittings have a fwhm of 1.2 eV. These BE values are indeed very similar to those on  $\text{Cu}(110)$  with 286.0 eV for  $\text{CH}_3\text{N}_2\text{CH}_3$  and 285.4 eV for  $\text{NCH}_3$  and  $\text{NCH}_2$ . At an annealing temperature of 450 K (Figure 3b), the amount of carbon still bonded to nitrogen and those already dissociated to form a silicon carbide species are almost equal. Some intensity between the two humps with a deconvoluted peak position of 284.5 eV indicates some  $\text{CH}_x$  intermediates prior to the Si-carbide formation. Finally at 600 K (Figure 3c),

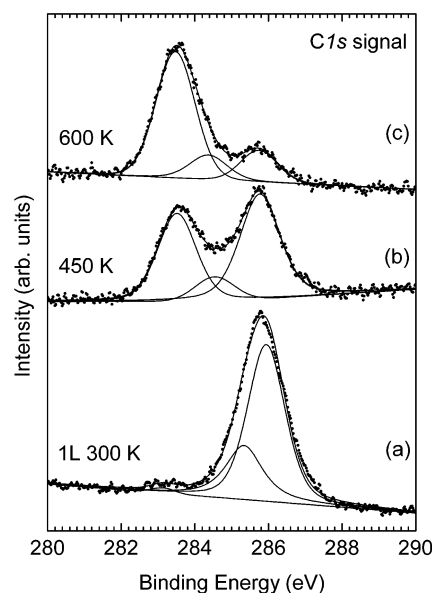


**Figure 3.** C 1s photoelectron spectra for  $\text{CH}_3\text{N}_2\text{CH}_3$  adsorbed on the  $\text{Si}(111)\text{-}7 \times 7$  surface taken at room temperature and at a photon energy of 512 eV: (a) 1 L adsorbed at 300 K, (b) after annealing to 450 K, and (c) after annealing to 600 K.

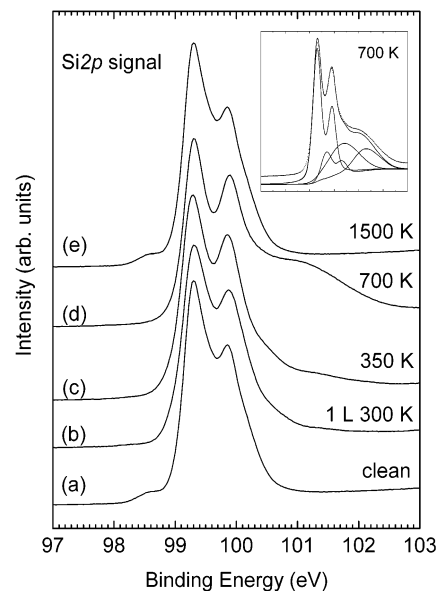


**Figure 4.** Si 1s photoelectron spectra for  $\text{CH}_3\text{N}_2\text{CH}_3$  adsorbed on the  $\text{Si}(111)\text{-}7 \times 7$  surface taken at room temperature and at a photon energy of 129 eV: (a) clean surface, (b) 1 L adsorbed at 300 K, (c) after annealing to 350 K, (d) after annealing to 700 K, and (e) after annealing to 1500 K. The insert shows spectrum d with peak analysis.

the majority of the remaining carbon species is present as Si-C with BE of 283.4 eV. This value is somewhat higher than the bulk value of SiC at 282.7 eV but consistent with values obtained after decomposition of azomethane on  $\text{Si}(100)$  at 283.3 eV<sup>9</sup> and methylhydrazine on  $\text{Si}(111)\text{-}7 \times 7$  at 283 eV.<sup>19</sup> The presence of a weak signal near 285.7 eV indicates that some  $\text{-N=N-}$  species, possibly in the form of  $\text{CH}_x\text{N}_2\text{CH}_y$ , still exist on the Si surface, again consistent with the HREELS spectra.

The Si 2p signal has been measured by tuning the photon energy to 129 eV, which is most surface sensitive with large excitation cross-section. The bottom spectrum of Figure 4 depicts the clean Si surface with characteristic spin-orbit splitting and a surface state at 98.5 eV attributed to the rest atoms contribution.<sup>25</sup> As expected, after deposition of 1 L

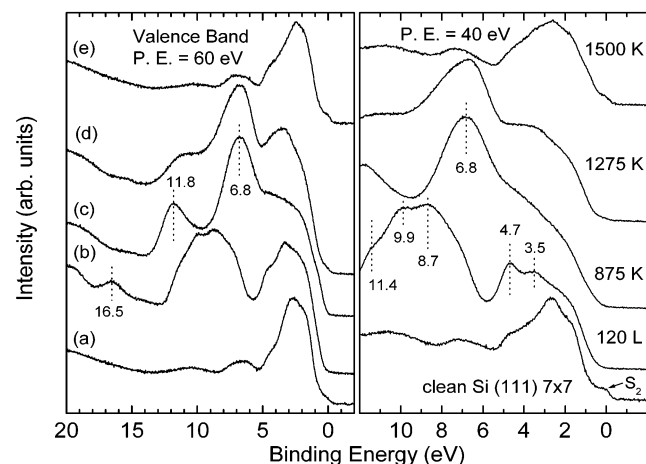


**Figure 5.** Valence band photoelectron spectra at photon energies of 60 (left) and 40 eV (right) with the same sequence: (a) clean Si(111)-7  $\times$  7, (b) exposed to 120 L azomethane at room temperature, (c) after annealing to 875 K, (d) after annealing to 1275 K, and (e) after annealing to 1500 K.

azomethane at 300 K, the surface state disappeared and a slight increase in background intensity toward higher BE can be observed. After annealing to 350 K, a hump at 101.3 eV BE becomes obvious. This agrees with the core level spectra of nitrogen and carbon, where the N 1s shows increasing Si nitridation at that temperature but C 1s does not display much change. At 700 K, the formation of nitride and carbide phases evolves, as indicated by the appearance of a very broad shoulder at higher BE (Figure 4d). The insert in Figure 4 gives a more detailed analysis of the components. The deconvoluted peaks include the bulk and surface components of the Si substrate and two broad peaks with centers at 100.4 and 101.3 eV BE, respectively. The peak at 100.4 eV fits well with the value for bulk SiC at 100.3 eV, while the component at 101.3 eV is close to the respective bulk Si<sub>3</sub>N<sub>4</sub> value of 101.8 eV. As inferred from the HREELS results, the Si-N phase at  $T = 700$  K is likely to exist in various chemical compositions on the surface. It is interesting to mention that after a single flash to the surface cleaning temperature of 1500 K, the Si 2p spectrum of the clean 7  $\times$  7 surface can be completely recovered (Figure 4e).

**3.2.2. Valence Band.** Figure 5 shows two series of valence band spectra obtained at photon energies of 60 and 40 eV, respectively. The bottom spectra are the clean Si(111)-7  $\times$  7 surface. After calibration of the photon energy, the BE scale has been aligned to the peak maximum of the surface state so-called S<sub>2</sub>.<sup>25,26</sup> The S<sub>2</sub> state originates from the rest atom dangling bonds (about 0.85 eV below the Fermi energy). After exposure of 120 L azomethane at 300 K, some prominent bands appear at 3.5, 4.7, 8.7, 9.9, 11.4, and 16.5 eV. As discussed in our previous study of azomethane adsorbed on the diamond surface,<sup>10</sup> the gas phase vertical ionization potentials of azomethane (around 9, 12, 14, 16, and 19 eV) are shifted downward upon adsorption and results in broad bands at about 5, 9, 12, and 15 eV BE relative to the Fermi edge. The UPS spectra of CH<sub>3</sub>N<sub>2</sub>H<sub>3</sub> on Si(111)-7  $\times$  7 exhibit bands at 4.4, 9.2, 10.7, and 16.2 eV.<sup>19</sup> The energy positions of these bands agree well with those in Figure 5b, assuming that the bands at 3.5 and 4.7 eV and the bands at 8.7 and 9.9 eV are sets of two bands with average energy positions at 4.1 and 9.3 eV, respectively. For the spectral assignments, we follow the interpretation of the gaseous azomethane spectra,<sup>27,28</sup> where the lowest energy band is due to the ionization from antibonding orbitals  $n_{-}$ . The bands around 12 eV (at 9 eV in the adsorbed

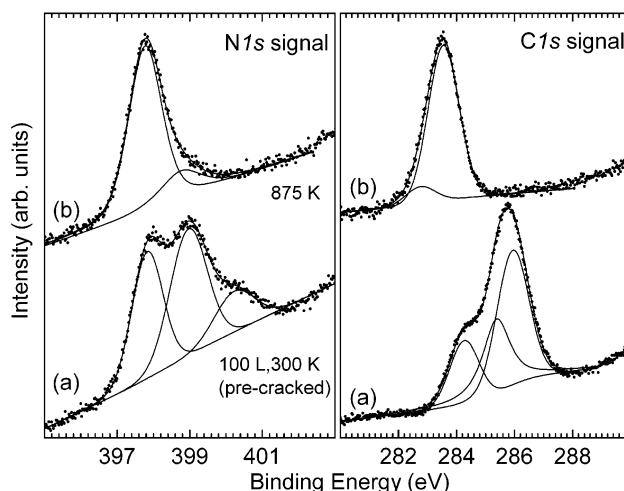


**Figure 6.** N 1s (left) and C 1s (right) photoelectron spectra of precracked CH<sub>3</sub>N<sub>2</sub>CH<sub>3</sub> adsorbed on the Si(111)-7  $\times$  7 surface taken at photon energies of 450 and 350 eV, respectively: (a) 100 L adsorbed at 300 K and (b) after annealing to 875 K.

case) can be assigned to bonding orbitals  $n_{+}$  and the  $\pi$ -molecular orbitals (MO) and the higher energy bands are likely associated with  $\sigma$ -MOs of the adsorbed molecules. From the results of HREELS and core level photoemission, we know the adsorbed molecules start to dissociate near 300 K. The rupture of N-N bonds for CH<sub>3</sub>N<sub>2</sub>H<sub>3</sub> on Si(111)-7  $\times$  7 is associated with the appearance of a very broad band spreading from 7 to 10 eV. Possible bands in this energy range for the dissociated species would overlap with bands from the intact molecule and be difficult to distinguish. However, it is very obvious that the spectra of Figure 5b are dominated by intensity between the two minima at 6 and 13 eV. It is therefore likely that the dissociated species contribute in this energy range. After annealing to 875 K, the formation of SiC and SiN layers is evident by two clear peaks at 11.8 and 6.8 eV and a shoulder around 4 eV. This agrees well with reported UPS data of SiC and SiN showing three bands at 3.5, 7.0, and 9.8 eV and 4.4, 7.0, and 11.2 eV, respectively.<sup>19</sup> The combination of both species leads to an intensity maximum around 7 eV as observed in Figure 5c. Further annealing to 1275 and 1500 K gradually recovers the clean Si surface (Figure 5d,e).

**3.2.3. Precracked Azomethane.** Although the conversion yield of azomethane into CH<sub>3</sub> and N<sub>2</sub> through pyrolysis is not complete, this thermal cracking technique generates an ideal source for CH<sub>3</sub> radicals to be used for chemisorption studies on many metal and diamond surfaces, due to the fact that azomethane, N<sub>2</sub>, and other hydrocarbon byproducts do not adsorb at 300 K on such surfaces. This is not the case on Si, where a strong interaction of azomethane and dissociated products with the substrate occurs at room temperature. However, an examination on precracked azomethane on Si can still provide further insights into the reaction mechanism on the surface. Figure 6 shows the N 1s and C 1s spectra for a dose of 100 L precracked CH<sub>3</sub>N<sub>2</sub>CH<sub>3</sub> adsorbed on the Si(111)-7  $\times$  7 surface and obtained at photon energies of 450 and 350 eV, respectively. As expected for the N 1s signal, the peak related to intact azomethane is strongly diminished and an increase in intensities of the dissociated species is observed. The peak center positions of the three components remain very much the same as compared to the nonprecracked exposure. After annealing to 875 K, 82% of the signal intensity originates from the Si-nitride component at 397.8 eV BE. The C 1s spectrum of precracked azomethane shows a new species at

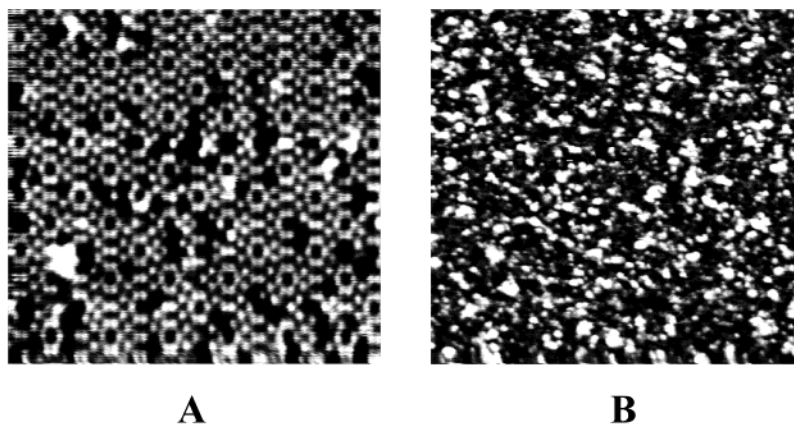


**Figure 7.** STM images of the Si(111) surface: (A) after exposure to 0.15 L azomethane at 300 K. Image size is 26.5 nm  $\times$  26.5 nm taken with a bias of +1.8 V and a tunneling current of 0.05 nA; (B) after exposure to 10 L azomethane at 300 K, followed by annealing to 1000 K. Image size is 110 nm  $\times$  110 nm taken with a bias of +2.0 V and a tunneling current of 0.15 nA.

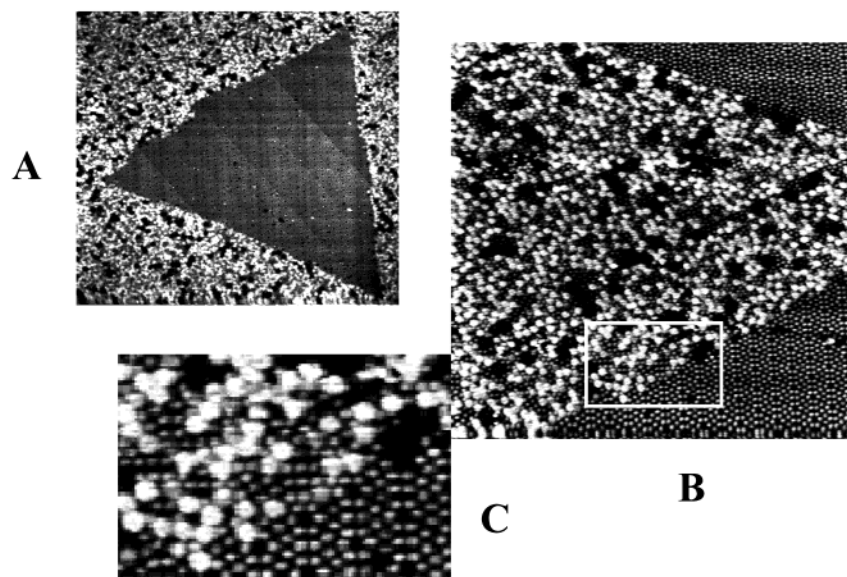


**Figure 8.** STM images of Si(111) surface after exposure to 10 L azomethane at 300 K, followed by annealing to 1500 K: (A) image size is 200 nm  $\times$  200 nm taken with a bias of +2.0 V and a tunneling current of 0.5 nA; (B) image size is 88 nm  $\times$  88 nm taken with a bias of +1.7 V and a tunneling current of 0.25 nA. (C) Enlargement of the selected area (white rectangular) in panel B.

284.3 eV besides the dominant peak at 285.9 eV and the shoulder at 285.4 eV. This new peak can be assigned to  $\text{CH}_3$  adsorbed on the surface. The radical species has been also detected for nonprecracked azomethane adsorption as intermediate after annealing to 450 K as seen in Figure 3b. Annealing to 875 K transforms all remaining carbon into Si-carbide with the emission peak centered at 283.6 eV BE. A small shoulder to even lower BE may due to a different stoichiometry of the Si-C phase. Therefore, the main effect of Si exposed to precracked azomethane is to enhance  $\text{CH}_3$  chemisorption at room temperature.

**3.3. STM Measurements.** The reconstructed Si(111)- $7 \times 7$  surface structure has been well-established experimentally and theoretically. The large unit cell and corrugation and the stability of the surface make this particular reconstruction a preferred object for STM studies, besides the fact that the structure is rather complicated<sup>29</sup> with various chemically distinguishable types of surface atoms. The reactivity of the surface in respect to adsorbed molecules depends on the local electronic configuration of the Si dangling bonds and on the molecule itself. The topographic STM image of the  $7 \times 7$  structure at positive sample bias shows 12 top layer adatoms in the unit cell. Upon adsorption of 0.15 L azomethane at room temperature, the

adatom structure is still visible. However, the change of electronic density due to the adsorbate is obvious from the appearance of dark and a few brighter areas (see Figure 7A). We do not observe at this stage any restructuring of the Si atoms. This is similar to a STM investigation by Yoshinobu and co-workers of acetylene on Si(111)- $7 \times 7$ .<sup>30</sup> Their detailed study on the adsorption site showed that the center adatoms were more reactive than the corner adatoms, and the molecule was proposed to be di- $\sigma$  bonded to the dangling bonds of a Si rest atom and an adjacent Si adatom. The suggestion for such bonding geometry was based on simple arguments by comparing the bond lengths of the molecule with the distance of two neighboring Si atoms possessing dangling bonds. Applying the same calculation for azomethane, we have to consider the N=N distance of 1.3 Å and the typical SiN bond length of 1.8 Å. If the molecule is di- $\sigma$ -bonded on the surface, the distance between the two Si atoms should be less than 4.9 Å. This can only be achieved by bridge bonding between a corner (or center) adatom and a rest atom with distances of 4.57 and 4.56 Å, respectively. The STM image shown in Figure 7A is complicated, however, by the fact that for the adsorbed azomethane on Si at 300 K, N=N bond scission occurs and only about 25% of the molecules are still intact according to the photoemission data. Figure 7B



displays the STM image after exposure to 10 L azomethane at 300 K and subsequent annealing to 1000 K. At this stage, only Si–C and Si–N species are present on the surface. Although no structural ordering can be detected, the surface retains a certain degree of homogeneity. Carbon and nitrogen are assumed to be bonded to Si in mixed phases.

By annealing to the surface-cleaning temperature of 1500 K, we find that the sample gradually recovers the  $7 \times 7$  structure forming characteristic triangles (see Figure 8). The sizes of the triangles can vary from 50 to 200 nm, and they increase with repetitive cycles of annealing, which finally result in the merging of neighboring triangles with stacking fault line. All of the triangles are oriented in the same way. The STM imaging of triangular-shaped structures has been reported previously for the Si(111)- $7 \times 7$  surface, e.g., after exposure to  $\text{SiH}_4$  to form Si(111)- $1 \times 1$ <sup>31</sup> and during the annealing process when the surface was quenched from high temperature.<sup>32</sup> The phase transition between  $(1 \times 1)$  and  $(7 \times 7)$  and the difference in density of those phases are considered to be the origin of the triangular domains.<sup>32</sup> In the study by Feenstra and Lutz<sup>33</sup> on the transformation of Si(111)- $2 \times 1$  to  $-7 \times 7$ , two intermediate states were identified, a disordered adatom-covered  $1 \times 1$  surface and a well-ordered  $5 \times 5$  structure. In the present study, we observe the triangular-shaped  $7 \times 7$  structure only when the surface has been exposed to azomethane prior to the annealing to 1500 K. We have never observed this structure during the regular cleaning process. Thus, the effect is not due to our annealing procedure but rather related to the surface chemistry. It is most likely that after the complete desorption of SiC and SiN species, the surface remains in a disordered phase of adatoms on top of a  $1 \times 1$  structure, similar to the intermediate states detected by Feenstra and Lutz.<sup>33</sup> This interpretation is supported by STM images as displayed in Figure 8B showing the area between two triangles. The enlarged region inside the rectangle (Figure 8C) reveals the underlying  $1 \times 1$  structure at the borderline to the reconstructed  $7 \times 7$ .

#### 4. Summary and Conclusions

The adsorption and thermal decomposition behavior of azomethane on Si(111)- $7 \times 7$  has been studied by HREELS, SR-PES, and STM. The major reaction steps deduced from the experimental data are summarized in the scheme depicted in Figure 9. At low-temperature exposure of 90 K, the molecule is adsorbed largely intact but with vibrational bands characteristic for both adsorption geometries, in trans form as well as cis form. It is likely that the pristine species adsorb on the  $7 \times 7$  surface by bridge bonding between a rest atom and a neighboring adatom according to the STM image and geometrical considerations. At an annealing temperature around 200 K, the molecules are partially dissociated with clear evidence of N=N bond breaking forming  $\text{NCH}_x$ . Other coadsorbates include H atoms and small amount of  $\text{CH}_x$  species based on HREELS spectra. Chemical decomposition of azomethane becomes more pronounced with the substrate at 300 K. At this temperature, a mixture of remaining intact azomethane,  $\text{NCH}_x$ , and Si– $\text{NH}_x$  species is evident on the surface. The Si–N species begins to appear as nitride, but essentially, no Si–C bonding is detected. The carbon on the surface is still attached to either nitrogen or hydrogen, in the forms of  $\text{NCH}_x$  and  $\text{CH}_x$ . Whereas N 1s PES spectra clearly exhibit three components at 300 K (indicated by the numbers 1–3 in Figure 9), C 1s shows only a broad peak of carbon related to the C–N=N–C and C–N bonding configurations. Judging from the absence of vibrational bands in the range of 1600–1700  $\text{cm}^{-1}$  and the corresponding

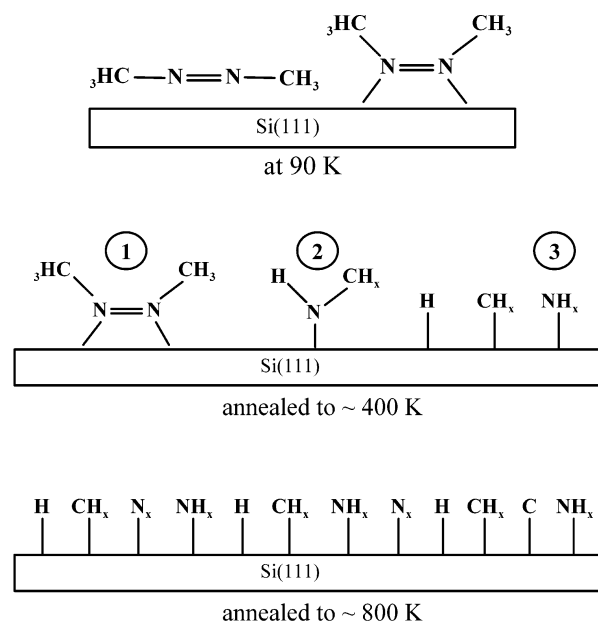


**Figure 9.** Adsorption and decomposition scheme of azomethane on the Si(111)- $7 \times 7$  surface at various temperatures.

photoemission spectra, we can conclude that azomethane does not undergo tautomerization with formation of C=N double bonds. At temperatures above 400 K, the remaining carbon can dissociate from nitrogen and react directly with the Si surface. This goes partially through the adsorption of  $\text{CH}_3$ , which is, however, only an intermediate for the Si–C formation.  $\text{CH}_3$  adsorption is strongly enhanced if azomethane is thermally precracked, which produces  $\text{CH}_3$  radicals prior to the exposure. At an annealing temperature of about 700 K, practically all surface carbon and nitrogen are bonded to Si, as clearly indicated by the Si 2p and valence band spectra. However, some hydrogen atoms are still attached to them and to the Si displaying the typical C–H, N–H, and Si–H vibrational bands. Finally, at 1000 K, the remaining hydrogen is desorbed and Si–C and Si–N phases are formed. In the case of nitrogen due to the limited supply of N atoms, different  $\text{Si}_x\text{N}_y$  compositions are likely and this may contribute to the broad HREELS band around 900  $\text{cm}^{-1}$ , which sharpens at higher annealing temperatures. After annealing to 1500 K, photoemission features typical for the clean Si(111)- $7 \times 7$  surface are immediately recovered. Si–C and Si–N species are desorbed in one flash, leaving a homogeneous but disordered surface with an underlying  $1 \times 1$  structure, which transforms back into the atomically less dense  $7 \times 7$  structure by forming triangular-shaped patterns as intermediate steps in the surface reconstruction process.

**Acknowledgment.** We thank S.-S. Gao, Ya-Ching Hou, Ping Chuang, and S.-C. Wang for technical help. We gratefully acknowledge the support of the Ministry of Education and the National Science Council of R.O.C. under Grant Nos. 90-N-FA01-2-4-5 and NSC 90-2112-M-213-003.

#### References and Notes

- (1) Chuang, T. J.; Chan, Y. L.; Chuang, P.; Klauser, R. *J. Electron. Spectrosc. Relat. Phenom.* **1999**, 98/99, 149 and references therein.
- (2) Weldon, M. K.; Friend, C. M. *Surf. Sci.* **1994**, 310, 94.
- (3) Jentz, D.; Trenary, M.; Peng, X. D.; Stair, P. *Surf. Sci.* **1995**, 341, 282.
- (4) Chuang, P.; Chan, Y. L.; Chuang, C. H.; Chien, S.-H.; Chuang, T. *J. Appl. Surf. Sci.* **2001**, 169, 153.
- (5) Bol, C. W. J.; Kovacs, J. D.; Chen, M.; Friend, C. M. *J. Phys. Chem. B* **1997**, 101, 6436.

- (6) Kis, A.; Barthos, R.; Kiss, J. *Phys. Chem. Chem. Phys.* **2000**, *2*, 4237.
- (7) Hanley, L.; Guo, X.; Yates, J. T. *J. Phys. Chem.* **1989**, *93*, 6754.
- (8) Castro, M. E.; Pressley, L. A.; White, J. M. *Surf. Sci.* **1991**, *256*, 227.
- (9) Loh, K. P.; Kingsley, C. R.; Foord, J. S.; Jackman, R. B. *Surf. Sci.* **1995**, *341*, 92.
- (10) Klauser, R.; Chuang, T. J.; Smoliar, L. A.; Tzeng, W.-T. *Chem. Phys. Lett.* **1996**, *255*, 32.
- (11) Rasko, J. *Appl. Catal., A* **2002**, *225*, 193.
- (12) Rochet, F.; Dufour, G.; Prieto, P.; Sirotti, F.; Stedile, F. C. *Phys. Rev. B* **1998**, *57*, 6738.
- (13) Mayne, A. J.; Avery, A. R.; Knoll, J.; Jones, T. S.; Briggs, G. A. D.; Weinberg, W. H. *Surf. Sci.* **1993**, *284*, 247.
- (14) Cheng, C. C.; Taylor, P. A.; Wallace, R. M.; Gutleben, H.; Clemen, L.; Colaizzi, M. L.; Chen, P. J.; Weinberg, W. H.; Choyke, W. J.; Yates, J. T. *Thin Solid Films* **1993**, *225*, 196.
- (15) Shimomura, M.; Munakata, M.; Iwasaki, A.; Ikeda, M.; Abukawa, T.; Sato, K.; Kawawa, T.; Shimizu, H.; Nagashima, N.; Kono, S. *Surf. Sci.* **2002**, *504*, 19.
- (16) Bu, Y.; Ma, L.; Lin, M. C. *J. Phys. Chem.* **1995**, *99*, 1046.
- (17) Bu, Y.; Ma, L.; Lin, M. C. *J. Phys. Chem.* **1993**, *97*, 11797.
- (18) Bacalzo-Gladden, F.; Lu, X.; Lin, M. C. *J. Phys. Chem. B* **2001**, *105*, 4368.
- (19) Bu, Y.; Shinn, D. W.; Lin, M. C. *Surf. Sci.* **1992**, *276*, 184.
- (20) Durig, J. R.; Pate, C. B.; Harris, W. C. *J. Chem. Phys.* **1972**, *56*, 5652.
- (21) Ackermann, M. N.; Craig, N. C.; Isberg, R. R.; Lauter, D. M.; Tacy, E. P. *J. Phys. Chem.* **1979**, *83*, 1190.
- (22) Colaizzi, M. L.; Chen, P. J.; Yates, J. T. *J. Chem. Phys.* **1992**, *96*, 7826.
- (23) Taguchi, Y.; Fujisawa, M.; Kuwahara, Y.; Onchi, M.; Nishijima, M. *Surf. Sci.* **1989**, *217*, L413.
- (24) Chuang, T. J.; Chan, Y. L.; Chuang, P.; Klauser, R.; Ko, C.-H.; Wei, D.-H. *Appl. Surf. Sci.* **2001**, *169/170*, 1.
- (25) Karlsson, C. J.; Landemark, E.; Chao, Y.-C.; Uhrberg, R. I. G. *Phys. Rev. B* **1994**, *50*, 5767.
- (26) Uhrberg, R. I. G.; Kaurila, T.; Chao, Y.-C. *Phys. Rev. B* **1998**, *58*, R1730.
- (27) Houk, K. N.; Chang, Y.-M.; Engel, P. S. *J. Am. Chem. Soc.* **1975**, *97*, 1824.
- (28) Brundle, C. R.; Robin, M. B.; Kuebler, N. A.; Barsch, H. *J. Am. Chem. Soc.* **1972**, *94*, 1451.
- (29) Takayanagi, K.; Tanishiro, Y.; Takahashi, S.; Takahashi, M. *J. Vac. Sci. Technol. A* **1985**, *3*, 1502.
- (30) Yoshinobu, J.; Fukushi, D.; Uda, M.; Nomura, E.; Aono, M. *Phys. Rev. B* **1992**, *46*, 9520.
- (31) Rauscher, H. *Surf. Sci. Rep.* **2001**, *42*, 207.
- (32) Yang, Y.-N.; Williams, E. D. *Phys. Rev. Lett.* **1994**, *72*, 1862.
- (33) Feenstra, R. M.; Lutz, M. A. *Surf. Sci.* **1991**, *243*, 151.